


RESEARCH

Open Access



# Human adipose and synovial-derived MSCs synergistically attenuate osteoarthritis by promoting chondrocyte autophagy through FoxO1 signaling

Jianqun Wu<sup>1,2</sup>, Songqiang Huang<sup>3</sup>, Yangyi Yu<sup>1,2</sup>, Qiang Lian<sup>1,2</sup>, Yang Liu<sup>4,5</sup>, Wenfeng Dai<sup>1,2</sup>, Qisong Liu<sup>1,2</sup>, Yonghao Pan<sup>4,5</sup>, Gui-ang Liu<sup>1,2</sup>, Kai Li<sup>4,5</sup>, Chao Liu<sup>4,5\*</sup> and Guangheng Li<sup>1,2\*</sup> 

## Abstract

**Background** Human adipose-derived stem cells (ADSCs) exert a strong anti-inflammatory effect, and synovium-derived stem cells (SDSCs) have high chondrogenic potential. Thus, this study aims to investigate whether a combination of human ADSCs and SDSCs will have a synergistic effect that will increase the chondrogenic potential of osteoarthritis (OA) chondrocytes in vitro and attenuate the cartilage degeneration of early and advanced OA in vitro.

**Methods** ADSCs, SDSCs, and chondrocytes were isolated from OA patients who underwent total knee arthroplasty. The ADSCs–SDSCs mixed cell ratios were 1:0 (ADSCs only), 8:2, 5:5 (5A5S), 2:8, and 0:1 (SDSCs only). The chondrogenic potential of the OA chondrocytes was evaluated in vitro with a transwell assay or pellet culture with various mixed cell groups. The mixed cell group with the highest chondrogenic potential was then selected and injected into the knee joints of nude rats of early and advanced OA stages in vivo. The animals were then evaluated 12 and 20 weeks after surgery through gait analysis, von frey test, microcomputed tomography, MRI, and immunohistochemical and histological analyses. Finally, the mechanisms underlying these findings were investigated through the RNA sequencing of tissue samples in vivo and Western blot of the OA chondrocyte autophagy pathway.

**Results** Among the MSCs treatment groups, 5A5S had the greatest synergistic effect that increased the chondrogenic potential of OA chondrocytes in vitro and inhibited early and advanced OA in vivo. The 5A5S group significantly reduced cartilage degeneration, synovial inflammation, pain sensation, and nerve invasion in subchondral nude rat OA, outperforming both single-cell treatments. The underlying mechanism was the activation of chondrocyte autophagy via the FoxO1 signaling pathway.

**Conclusion** A combination of human ADSCs and SDSCs demonstrated higher potential than a single type of stem cell, demonstrating potential as a novel treatment for OA.

**Keywords** Adipose-derived stem cells, Synovium-derived stem cells, Osteoarthritis, Autophagy, Cartilage regeneration

<sup>†</sup>Jianqun Wu and Songqiang Huang have contributed equally to this work.

\*Correspondence:

Chao Liu

liuc33@sustech.edu.cn

Guangheng Li

liguangheng@hotmail.com

Full list of author information is available at the end of the article



## Introduction

Osteoarthritis (OA) is one of the most common causes of chronic pain and musculoskeletal disability, and it has recently categorized as an epidemic, put a substantial burden on the healthcare system [1]. OA is characterized by persistent inflammation and progressive articular cartilage degeneration, subchondral bone remodeling, and osteophyte formation [2]. Nonpharmacological approaches (such as exercise and weight management) and pharmacological interventions (including nonsteroidal anti-inflammatory drugs) constitute clinical guidelines for nonsurgical OA treatment. Nonsurgical treatments relieve symptoms by reducing inflammation but do not repair damaged chondrocytes or regenerate the cartilage matrix [1, 3].

Comprehensive therapies that can suppress inflammation while promoting cartilage regeneration may delay or prevent the progression of OA [4]. Mesenchymal stem cells (MSCs)-based therapy has attracted considerable interest because of its potential for anti-inflammatory and regenerative effects [5, 6]. Autologous MSCs therapy improves knee pain, self-reported physical function, and cartilage quality [7, 8]. MSCs can be isolated from various tissues, including bone marrow-derived stem cells (BMSCs) [9], adipose tissue-derived stem cells (ADSCs) [10], and synovium-derived stem cells (SDSCs) [11]. However, MSCs from various tissues have distinct functional characteristics [12] and have vary therapeutic outcomes [13, 14]. Compared with BMSCs, ADSCs have robust proliferation and anti-inflammatory effects but limited chondrogenic potential [10, 13]. In animal models and clinical trials, ADSCs substantially reduce inflammatory mediators, such as tumor necrosis factor  $\alpha$  (TNF- $\alpha$ ) and interleukin-1 $\beta$  (IL-1 $\beta$ ) [15, 16]. Meanwhile, SDSCs have demonstrated greater chondrogenic potential than BMSCs, ADSCs, periosteum, and muscle-derived stem cells [12, 17, 18]. Chondrocytes cocultured with SDSCs express higher genes levels of *Col2* and *Sox9* and lower levels of *Col1* and *Col10* than chondrocytes alone, indicating that SDSCs promoted chondrogenesis while inhibiting hypertrophy [19]. Furthermore, at the 24-month follow-up, autologous SDSCs implantation outperforms chondrocyte implantation in terms of functional outcomes and OA outcome scores [20]. Thus, SDSCs have a remarkable potential for cartilage regeneration.

Intra-articular injections of ADSCs or SDSCs have demonstrated limited efficacy in advanced OA and long-term therapeutic applications [21]. MSCs-based therapies for OA frequently combine MSCs with bioactive molecules or scaffolds to increase their therapeutic potential, resulting in improving stem or progenitor cell homing, reducing enzymatic matrix degradation and inflammation [22]. The benefits of MSCs derived from

different tissues, such as ADSCs' anti-inflammatory effects and SDSCs' cartilage regeneration potential, have prompted investigations on combined approaches using multiple MSCs sources, offering a novel treatment paradigm that may be superior to single-MSCs therapies [23]. The aim of this study was to test the hypothesis that intra-articular injection of a combination of ADSCs and SDSCs would have a synergistic effect on reducing inflammation and promoting the regeneration of cartilage in OA. We expected that this combination therapy would lead to therapeutic outcomes surpassing those obtained using ADSCs or SDSCs alone.

## Materials and methods

### Isolation and cultivation of human chondrocytes, ADSCs, and SDSCs

Femoral condyles, synovial tissues, and infrapatellar fat pad (IPFP) were aseptically harvested from patients after total knee arthroplasty (TKA). The procedure was approved by the medical ethics committee of Shenzhen People's Hospital (LL-KY-2021069). The following inclusion criteria were used: 1) primary knee OA and TKA, 2) age of less than 70 years. The exclusion criteria were as follows: (1) rheumatoid arthritis, (2) concurrent conditions, such as inflammation, suspected infection, or diabetes. The patients comprised 6 male patients and 12 female patients, ranging in age from 38 to 68 years. All specimens underwent triple rinsing with PBS supplemented with a penicillin-streptomycin solution (PS; 100 units/ml penicillin, 100  $\mu$ g/ml streptomycin, Gibco). Briefly, (1) cartilage samples (weight 6–8 g) as pieces digested with 0.5% protease (Sigma) for 30 min and 0.05% type II collagenase (Sigma) for 6 h. (2) IPFP and synovial tissue (weight 5–6 g) were digested with 0.075% type XI collagenase (Life Technologies) on a 37 °C shaker for 1 h (Fig. S1A). After passing through a 100  $\mu$ m strainer, the suspension was centrifuged at 800 $\times$ g for 5 min. Cells were resuspended and cultured in 10 cm<sup>2</sup> plates in Dulbecco's modified eagle medium/nutrient mixture F-12 (DMEM/F12, Gibco) supplemented with 15% fetal bovine serum (FBS, Gibco) and PS. Cultures were maintained at 37 °C and 5% CO<sub>2</sub>, and the medium was replaced every 2–3 days until the cells reached 70–80% confluence. ADSCs and SDSCs cultures were incubated until the third passage for experiments.

### Coculture of chondrocytes with combined SDSCs and ADSCs

As described previously, ADSCs have a strong anti-inflammatory effect, whereas SDSCs have a strong chondrogenic potential. To establish mixed MSCs with most protective effects of both anti-inflammatory and pro-cartilage regeneration, different ratios of mixed

ADSCs and SDSCs, as 2:8, 5:5, 8:2, were established (Extended Data Table 1). Chondrocytes ( $2 \times 10^5$ ) were centrifuged at  $800 \times g$  for 5 min to form a chondrocyte pellet. Those pellets were then randomly placed in the upper chamber and indirectly cocultured with  $2 \times 10^5$  SDSCs alone or ADSCs alone or both in various ratios in the lower chamber. In the 3D pellet directly co-culture system comprising  $2 \times 10^5$  chondrocytes and  $2 \times 10^5$  SDSCs and ADSCs at different ratios, the control group was composed of  $4 \times 10^5$  chondrocyte only, all cells were centrifuged at  $800 \times g$  for 5 min to form a 3D pellet. The chondrogenic medium was changed every other day for 14 days. The maximum diameter was observed and measured by a dissecting microscope, the pellets were dehydrated and paraffin embedded for paraffin sections. The proliferation potential of chondrocytes cocultured with SDSCs and ADSCs by transwell system, and immunofluorescence were performed after 5 days.

#### Conditioned medium

The third passage total  $6 \times 10^5$  cells of ADSCs only,  $6 \times 10^5$  cells of SDSCs only, mixed  $3 \times 10^5$  ADSCs and  $3 \times 10^5$  SDSCs were cultured in a  $10 \text{ cm}^2$  dish, the culture medium was changed after 24 h, and the conditioned medium was collected after another 48 h. The conditioned medium was centrifuged at  $800 \times g$  for 5 min, filtered through  $0.2 \mu\text{m}$  filter, and stored at  $-80^\circ\text{C}$ .

#### IL-1 $\beta$ induced chondrocyte culture in vitro

Chondrocyte was cultured with IL-1 $\beta$  at a concentration of  $10 \text{ ng}/\mu\text{L}$  for 48 h. The medium was changed to SDSCs or ADSCs, or 5A5S conditioned medium or 5A5S conditioned medium with  $0.1 \mu\text{M}$  AS184285(AS), a specific Foxo1 inhibitor (MedChemExpress), cultured for 72 h. Finally, cell were performed for western blotting, immunofluorescence and mono-dansylcadaverine staining.

#### Electron microscopy analysis

For electron microscopy,  $2.0 \times 10^6$  chondrocytes were collected by centrifugation and fixed for 24 h at  $4^\circ\text{C}$  in a transmission electron microscopy (TEM) fixative. After fixation, the samples were dehydrated in graded alcohols, infiltrated in epoxypropane, and embedded in Embed 812. Ultrathin  $60 \text{ nm}$ -thick sections were created and fished out onto the  $150$  meshes cuprum grids with Formvar film. A 2% uranium acetate saturated alcohol solution staining for 8 min, rinsed in 70% ethanol three times. Lead citrate staining was performed for 8 min. After drying with filter paper, the cuprum grids were placed in a grid board and dried overnight at room temperature. The cuprum grids were observed through TEM, and images were obtained.

#### Nude rat OA model and animal groups

Male athymic nude rats (aged 10–12 weeks, body weight, 160–180 g,  $n=41$ ) were obtained from Vital River Laboratory Animal Technology (Beijing, China), which is known for lower immunological rejection and higher success rates of transplantations. All experimental and animal care procedures were approved by Southern University of Science and Technology (SUSTech-SL2021112901). The work has been reported in line with the ARRIVE guidelines 2.0. All rats were induced by inhalation of isoflurane (concentration as 3–4%) through a mask for 2–3 min, and then the concentration was changed to 2–3% for the maintenance of anesthesia. As nude rats difficult to breed and really expensive than Sprague–Dawley rats, a bilateral OA model was established by partial medial meniscectomy (pMMx). The experimental rats were randomly assigned into six groups ( $n=10$ ): PBS group (OA with  $50 \mu\text{l}$  of PBS), ADSCs-only group (OA with  $1.0 \times 10^6$  ADSCs), SDSCs-only group (OA with  $1.0 \times 10^6$  SDSCs); 5A5S group (OA with  $5 \times 10^5$  ADSCs and  $5 \times 10^5$  SDSC) [15, 24, 25]. Mild and advanced OA progressed 4 and 12 weeks after pMMx, respectively. In order to avoid the weight bearing asymmetry of gait, different treatments in bilateral OA, as PBS in left OA and ADSCs in right OA, SDSCs in left OA and 5A5S in right OA. PBS or cells was injected into rats in the mild OA group 4 weeks after pMMx and then performed every 4 weeks for 12 weeks ( $n=6$ ). As for the advanced group, injection started 12 weeks after pMMx and then performed every 4 weeks for 20 weeks ( $n=4$ ). Different proportions of mixed ADSCs and SDSCs were pooled from same patient at each knee injection. But at different time points, different patient-derived cells were pooled with little heterogeneity under inclusion and exclusion criteria [26]. The sham group had surgery and only underwent arthrotomy in the same surgical incision and suture. Those rats were euthanized by cervical dislocation at 12 or 20 weeks. The knee joints were assessed by microcomputed tomography (micro-CT), MRI, and immunohistochemical and histological analyses.

#### Gait analysis and von frey testing

Rats were trained for 30 min on a transparent Plexiglass walking track or a perforated metal floor (Ugo Basile) before testing. Gait analysis was conducted using a catwalk system (Noldus CatWalk XT), and foot gait data were collected. Von frey testing started with the von frey filament (15 g) and then decreased to 10 g or increased to 26, 60, 100, and 180 g, according to whether rapid paw withdrawal occurred. The mechanical pain threshold was calculated by the up-down Excel program (Dixon, 1965).

### MRI analysis

All imaging experiments were carried out on a 9.4 Tesla bore magnet MRI scanner ( $\mu$ MR 9.4 T, United imaging Life Science Instruments, China). A fat-suppressed high-resolution proton density weighted fast spin echo sequence were acquired in the sagittal and coronal planes. The parameters were set as follows: TE/TR=15.36 ms/2000 ms, ETL=5, field of view=18×38 mm<sup>2</sup>, matrix size=176×372, slice thickness=1 mm, slice gap=0 mm, voxel size=0.1×0.1×1 mm<sup>3</sup>, number of averages=2.

### X-ray and micro-CT analysis

All knee joints underwent X-ray and micro-CT with Sky-Scan1178 (Bruker microCT, Kontich, Belgium). X-ray images were captured from the knee joints in the anteroposterior position with following parameters: 100 kV (voltage), 200  $\mu$ A (current), 10  $\mu$ m (resolution), and 623 ms (exposure time). The subchondral bone was analyzed in terms of bone volume per tissue volume (BV/TV), trabecular thickness (Tb.Th) and structure model index (SMI). Representative three sections (coronal, sagittal, and transverse section) of each group were generated using DataViewer (Bruker micro-CT).

### Macrography and histological analysis

Gross morphological changes in the articular cartilage were photographed by close-up microlens and assessed according to predefined criteria [27]. The samples were fixed in 4% paraformaldehyde for 24 h and decalcified in 10% ethylenediaminetetraacetic acid for 6 weeks, and then embedded in paraffin. Sagittal sections (6  $\mu$ m thick) were obtained from the medial to the middle regions with a rotary microtome (Leica, Germany). Paraffin sections were stained with Hematoxylin and eosin (H&E) kit (Solarbio, China) or Safranin O/Fast Green kit (SO&FG, Solarbio, China). All sections were scanned under a microscope (Leica, aperio versa 8). Lesions in the cartilage were blindly assessed by two independent researchers based on the a 0–24 scale classification system [28].

### Immunohistochemical analysis

After deparaffinization and rehydration, the paraffin sections were immersed in boiled citrate buffer solution (pH 7.4) for 8 min for antigen retrieval. Then, the sections were blocked with 3% hydrogen peroxide for 25 min and 3% BSA for 30 min. A primary antibody in a certain proportion (anti-MMP-13, anti-Col2, and anti-IL-1 $\beta$ ) was added to the sections, which were incubated overnight at 4 °C. The sections were then covered with corresponding secondary antibodies and incubated at room temperature for 60 min. DAB color developing solution was added and until the color developed as brownish yellow. The

staining percentage area for the IHC marker of MMP-13, Col2 and IL-1 $\beta$  were measured with a semi-quantitative method using ImageJ [24]. For IHC percentage determination, regions of interest were detected and defined. Then, the image was adjusted through red color segmentation (RGB mode), and the color thresholds for hue, saturation, and brightness were set. This threshold was identical in all biological and technical replicates within each IHC marker. Finally, the average optical density was calculated and obtained by integrated optical density/VOI area. Positive cells were counted or the area of the marker proteins were measured in three areas in each slide, and each group had three sections.

### RNA sequencing and data analysis

Cartilage samples were harvested from the medial tibial plateau in the sham, PBS, and 5A5S groups (n=3) at 20 weeks. RNA was lysed with Trizol reagent and quantified with ND-2000 (NanoDrop Technologies). A sequencing library was constructed using BGISEQ-500 (igenecode Biotech, Beijing), and qualified reads were mapped to the rat reference genome. Differential expression analysis between groups was performed using the DESeq2 R package. Differentially expressed genes (DEGs) were defined as having a log<sub>2</sub> fold change  $\geq 2$  and *P* value  $\leq 0.05$ . Heat maps were generated using the heatmap package. Gene ontology (GO) enrichment analysis and KEGG pathway analysis were performed using cluster Profiler R package.

### Statistical analysis

Data were expressed as means  $\pm$  SD and analyzed with GraphPad Prism (version 9.0; GraphPad Software, California). Intergroup comparison was subject to one-way analysis of variance followed by Tukey post-hoc tests. Statistical significance was set at *P* < 0.05.

## Results

### Combined ADSCs and SDSCs promoted cartilage tissue formation in vitro

Femoral condyle, IPFP, and synovial tissues were harvested from patients with TKA (Fig. S1, A). Chondrocyte, ADSCs, and SDSCs exhibited a typical spindle-shaped phenotype (Fig. S1, A). The differentiation potential of the ADSCs and SDSCs toward adipocytes, osteoblasts, and chondrocytes were demonstrated using corresponding induction media for 14 days. ADSCs exhibited a remarkable red oil droplet by oil red o staining, whereas induced SDSCs displayed obvious mineralization deposition by alizarin red s staining and abundant glycosaminoglycan deposition through alcian blue staining (Fig. S1, B). Flow cytometry analyses revealed that the SDSCs and ADSCs were highly positive for CD73, CD44, CD90, and

CD105 and negative for CD45 and CD34 (Fig. S1, C). The cells were verified as multipotent MSCs.

Different proportions of ADSCs and SDSCs were cocultured with chondrocytes in vitro by transwell for 14 days during chondrogenic differentiation (Fig. 1A, B). The diameters of the chondrocyte pellets in the 8A2S and 5A5S groups were larger than those in the control group (Fig. 1C, D). Additionally, the proteoglycan glycans and Col2 expression levels in the SDSCs-only, 8A2S, 5A5S, and 2A8S groups were higher than those in the control group, and the 5A5S groups

showed the largest improvement (Fig. 1E–H). Furthermore, the direct contact 3D pellets including ADSCs, SDSCs and chondrocytes also demonstrated that 8A2S, 5A5S enhanced cartilage regeneration (Fig. S2, A–D). Combined ADSCs and SDSCs promoted the proliferation of chondrocytes, increasing the number of Ki67 positive cells (Fig. 1I, J). These results suggested that the combined ADSCs and SDSCs promoted cartilage tissue formation. The 5A5S group exhibited the largest synergistic effect that promoted cartilage tissue formation.

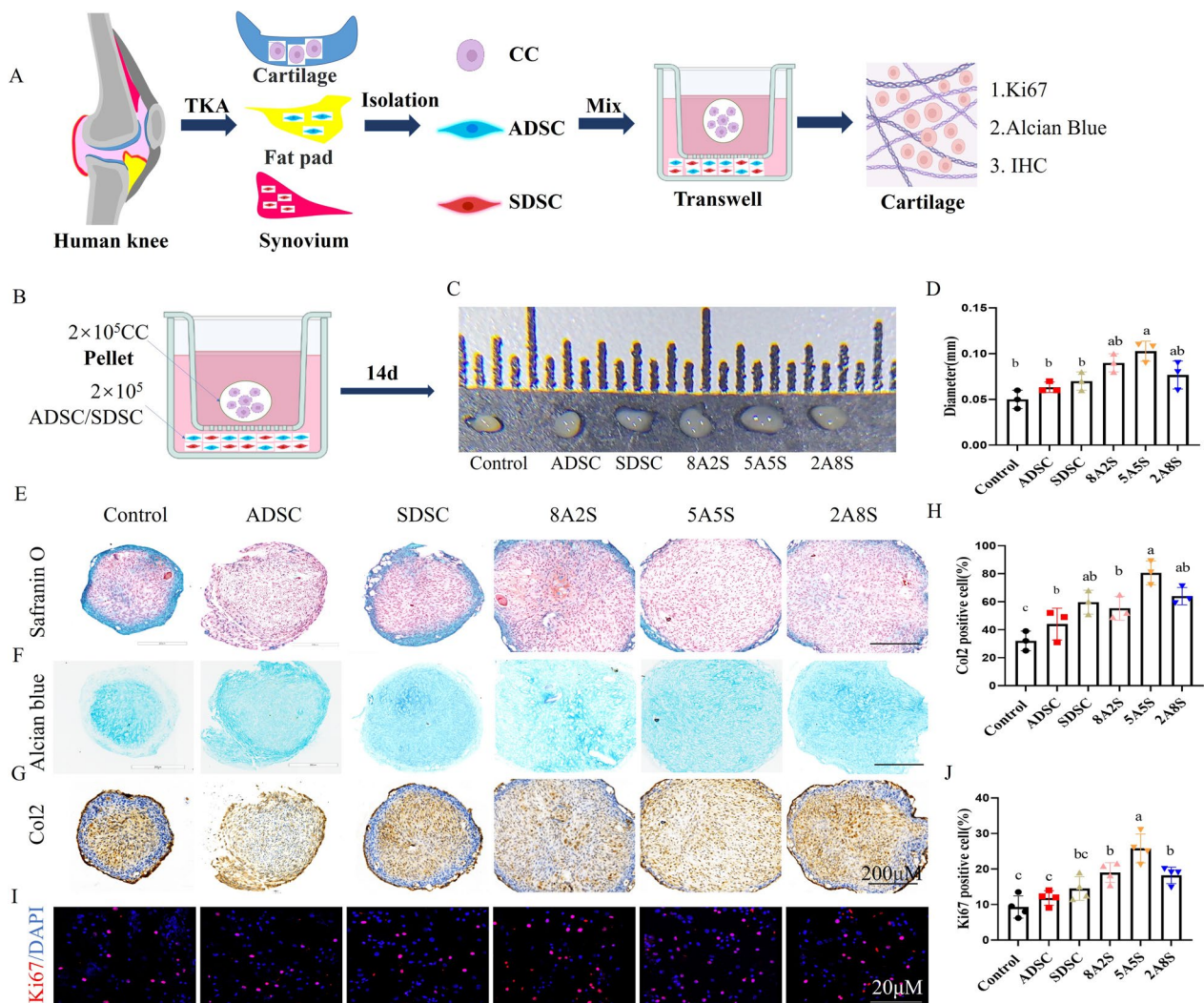


**Fig. 1** Mixed ADSCs and SDSCs treatments promoted cartilage tissue formation and proliferation of chondrocytes. **A** schematic diagram of the combined MSCs treatment for chondrocyte. **B** schematic illustration of chondrocyte pellet cocultured with mixed ADSCs and SDSCs. **C** the chondrocyte pellet of gross view and quantitative analysis of diameter (**D**). **E** Safranin O staining, **F** Alcian blue staining, **G** Col2 immunohistochemical staining for pellet and **H** quantitative analysis of the Col2-positive cells. **I**, evaluation of the proliferation of chondrocytes by Ki67 and **J** the proportion of Ki67 positive cells. (TKA, total knee replacement; CC, chondrocyte; ADSC, adipose-derived stem cells; SDSC, synovium-derived stem cells. All data are shown as the mean  $\pm$  SD. n = 3 or 4)

**Retention and distribution of ADSCs and SDSCs in articular cavity after intra-injection**

To explore how long the ADSCs or SDSCs reside in OA, ADSCs or SDSCs labeled with second near infrared (NIR-II) fNPs was determined [29]. The viability of the fNP-labeled ADSCs or SDSCs was similar to the unlabeled ADSCs or SDSCs (Fig. S3A, B). fNP-labeled ADSCs or SDSCs were injected into the OA at 4 weeks after pMMx. The NIR-II signals in the knee were observed at 0, 1, 3, 4, 8, and 12 weeks after injection and were standardized to the fluorescence intensity at day 0. The fluorescence intensity decreased to  $18.4 \pm 2.1\%$  at 4 weeks after injection and continued to decrease until 12 weeks. The fNPs alone disappeared completely at 4 weeks (Fig. 2A, B). Out of the total transplanted SDSCs or ADSCs, 95–99% were distributed in the synovial membrane and meniscus, whereas 1–5% were distributed in the damaged

cartilage at 12 weeks after injection (Fig. 2C, D). Immunohistochemical staining of anti-human nuclear antigen, which specifically labeled human-derived cells, revealed the presence of implanted human-derived SDSCs or ADSCs in the synovial membrane, meniscus and cartilage (Fig. S3C, D).

**Equal amounts of ADSCs and SDSCs synergistically improved knee pain, gait and subchondral bone remodeling in early or advanced OA**

Four or twelve weeks after pMMx developed as early OA (Fig. S4A, B) or advanced OA phenotype. ADSCs or SDSCs or a combination ADSCs and SDSCs in equal amounts were intra-injected in OA every 4 weeks for twice (Fig. S5A). None of the rats exhibited wound infection, knee joint infection and mortality. Compared with the PBS group, the representative signal images of gait

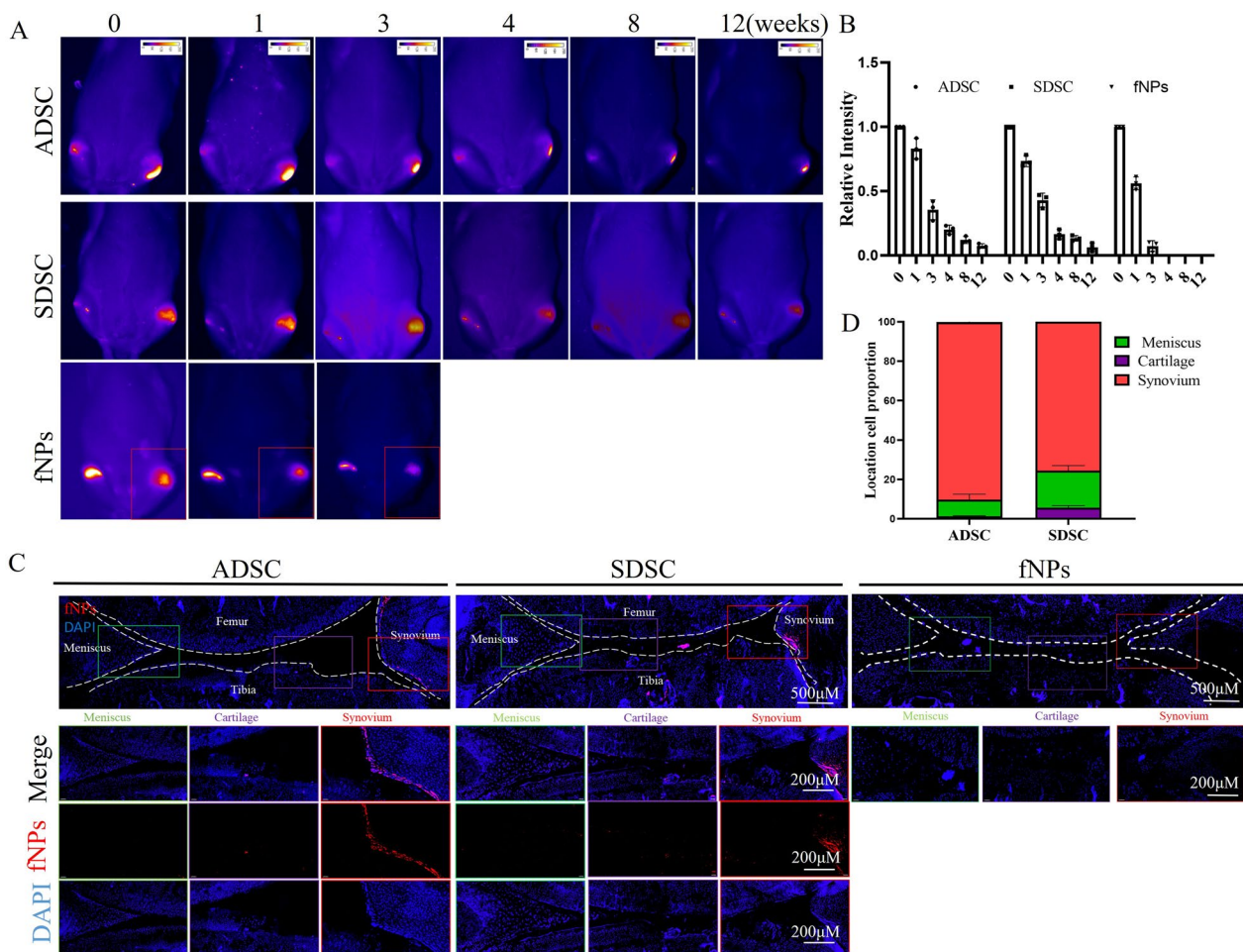


**Fig. 2** Long-term tracking of ADSCs or SDSCs in rat joints. **A** fNP-labeled ADSCs or SDSCs residing in the knee joint with NIR-II imaging during 0–12 weeks. **B** quantification of the fluorescence intensity of fNP-labeled ADSCs or SDSCs in the knee joint. **C** confocal microscopy of fNP labeled ADSCs or SDSCs in knee at 12 weeks, fNP only at 4 weeks, and zoomed-in images of regions in synovial membrane, meniscus and cartilage. (All data were shown as the mean  $\pm$  SD, n=3)

showed that the mean print area and mean intensity of the hind foot considerably improved in the SDSCs only at 12 weeks and in 5A5S groups at 12 and 20 weeks (Fig. S5B, C). In the PBS-treated rats, the paw withdrawal pain threshold of the OA knee markedly decreased at 8, 12 and 20 weeks. By contrast, pain threshold greatly increased in the ADSCs at 8 weeks and 5A5S at 12 and 20 weeks (Fig. S5D). The proportion and area of the CGRP<sup>+</sup> nerve in the subchondral bone were decreased in the 5A5S groups at 12 and 20 weeks (Fig. S5E, F).

After twice MSCs treatments for early OA at 12 weeks or for advanced OA at 20 weeks respectively (Fig. 3A). Macroscopic observations showed a severe OA features at 12 weeks, such as erosions and defects of articular surface in the PBS group, and indicated a larger erosions and defects of articular cartilage at 20 weeks. The 5A5S groups displayed smoother surfaces with fewer erosions and lower macroscopic scores than the other groups, suggesting less severe progression of OA (Fig. 3B, C). Micro-CT 3D reconstruction and subchondral bone analysis indicated large defects in the subchondral bone in the PBS group at 12 weeks and worsened at 20 weeks, the SDSCs or ADSCs alone group showing less subchondral bone damage than the PBS group, the smallest degree of damage was observed in the 5A5S groups (Fig. 3D, F). Besides, 5A5S groups showed lower BV/TV, Tb.Th, and higher SMI than PBS groups at 12 weeks, 5A5S groups showed lower BV/TV, Tb.Th, and higher SMI than those in PBS, SDSCs alone and ADSCs alone groups at 20 weeks (Fig. 3E, G, I). MRI images showed the high signal intensities of large bone cysts and severe cartilage swelling in the PBS group, and the ADSCs or SDSCs-only groups showed some cartilage swelling. The signal intensity of cartilage in the 5A5S groups was considerably smooth without bone cysts and cartilage swelling (Fig. 3H). Together, these findings suggested that combined ADSCs and SDSCs attenuated bone remodeling. Meanwhile, ADSCs, SDSCs alone treatments decelerated the formation of osteophytes around the knee joint at 12 and 20 weeks, and 5A5S treatments reduced the BV of osteophytes than ADSCs or SDSCs alone group at 20 weeks (Fig. 4J, K). These results suggested that combined MSCs treatments were more effective in attenuating subchondral bone remodeling and osteophyte formation in advanced OA than treatments with a single type of ADSCs or SDSCs.

### Equal amounts of ADSCs and SDSCs synergistically relieved cartilage degeneration and inflammation

Cartilage degeneration and synovial inflammation in mild or advanced OA after MSCs treatments were evaluated by H&E staining, Safranin O–Fast Green staining and immunohistochemistry (Fig. 4A). As illustrated in Fig. 4, cartilage degeneration in the PBS group exhibited substantial loss in hyaline cartilage thickness, proteoglycans and Col2 protein expression at 12 weeks, and cartilage destruction aggravated and penetrated the subchondral bone at 20 weeks. ADSCs and SDSCs alone treatment prevented the OA-induced decreases in hyaline cartilage thickness at 12 weeks (Fig. 4B, C), and in proteoglycans with high OARSI scores at 12 and 20 weeks (Fig. 4D, E) and in Col2 protein expression at 12 weeks (Fig. 4F, G), extraordinary, 5A5S have a more protective effect than ADSCs and SDSCs alone in hyaline cartilage thickness at 12 weeks, proteoglycans at 12 and 20 weeks and Col2 protein expression at 12 weeks (Fig. 4B–G). Compared with the PBS groups, the 5A5S groups significantly decreased the proportion of positive MMP13 cells at 12 and 20 weeks (Fig. 4H, I). Furthermore, ADSCs alone and 5A5S reduced synovial inflammation indicated by markedly decreased in synovitis score (Fig. 4J, K) and proportion of IL-1 $\beta$  positive cells (Fig. 4L, M). These results suggested that combined MSC treatments were more effective in attenuating cartilage degeneration in advanced OA than ADSCs and SDSCs alone.

### Chondrocyte autophagy and FoxO signaling pathway were involved in the cartilage regeneration in advanced OA after the treatments of ADSCs and SDSCs

The molecular mechanisms of cartilage degeneration alleviation by using mixed MSCs in equal proportions were evaluated. We identified DEGs in the cartilage tissue samples at 20 weeks through RNA sequencing and analysis (Fig. 5A). Principal component analysis (PCA) of the gene expression profile showed a significant separation between the PBS and sham groups. Compared with the PBS group, the 5A5S cluster was closer to the sham group, indicating that the gene expression of 5A5S group was more similar to the sham group (Fig. 5B). A total of 626 DEGs between 5A5S and PBS were identified for further analysis in the cartilage tissues. A total of 393 genes were down-regulated and 233 genes were up-regulated

(See figure on next page.)

**Fig. 3** A combination of ADSCs and SDSCs in equal amounts improved the subchondral bone and osteophytes changes in early and advanced OA. **A** schematic illustration of intra-injection of ADSCs and SDSCs for OA therapy. **B** the gross view of the tibial articular surface and macroscopic scores (**C**) ( $n=3$ ). **D** 3D reconstruction of subchondral bone, **E** BV/TV, **G** Tb.Th and **I** SMI for medial subchondral bone ( $n=6$  or 4). **F** coronal view of subchondral bone. **H** subchondral bone cyst (blue arrow) and cartilage edema (red arrow) by MRI images. **J** 3D reconstruction (marked in red) and **K** bone volume of the osteophytes around the knee joint ( $n=4$ ). All data are shown as the mean  $\pm$  SD

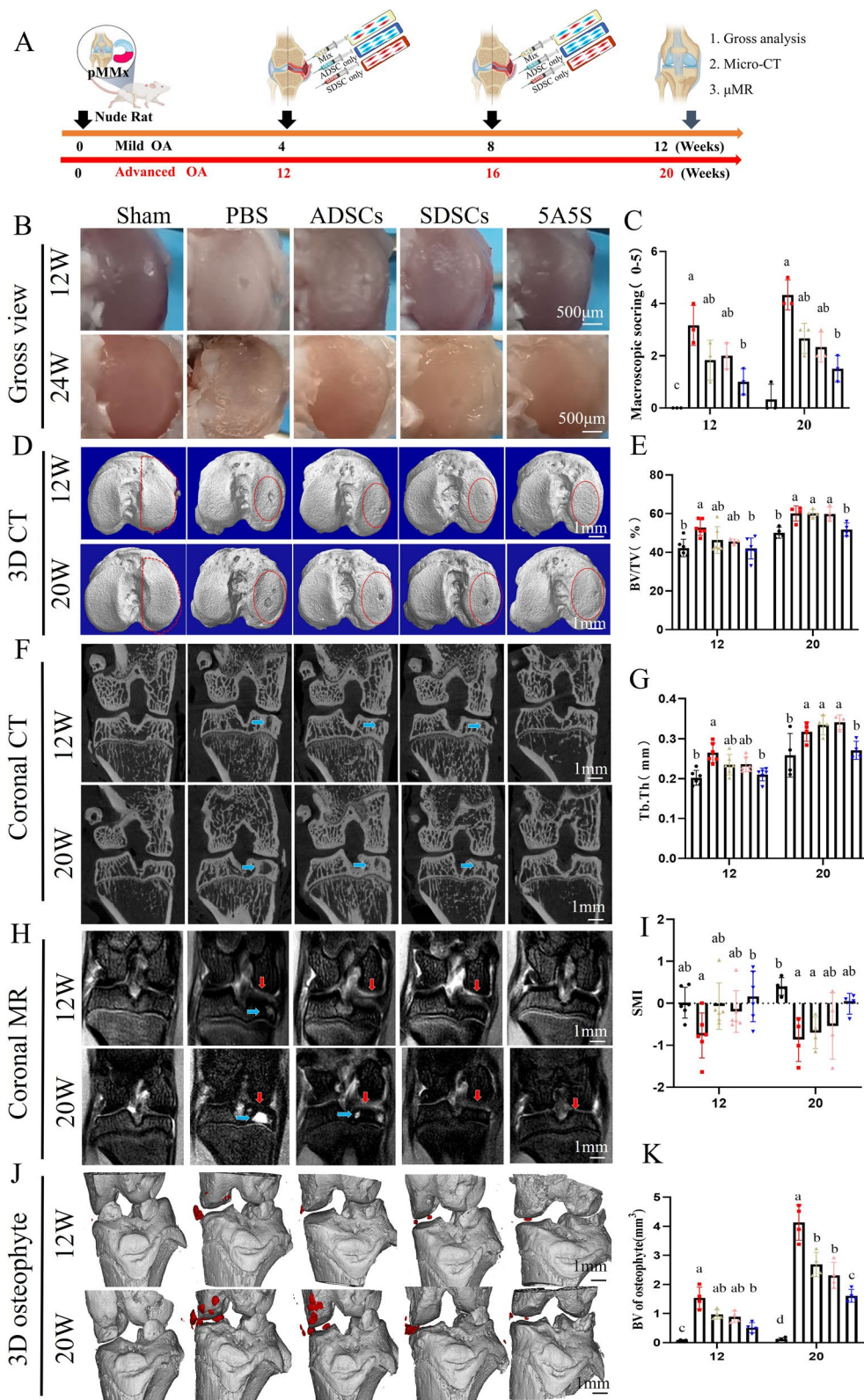


**Fig. 3** (See legend on previous page.)



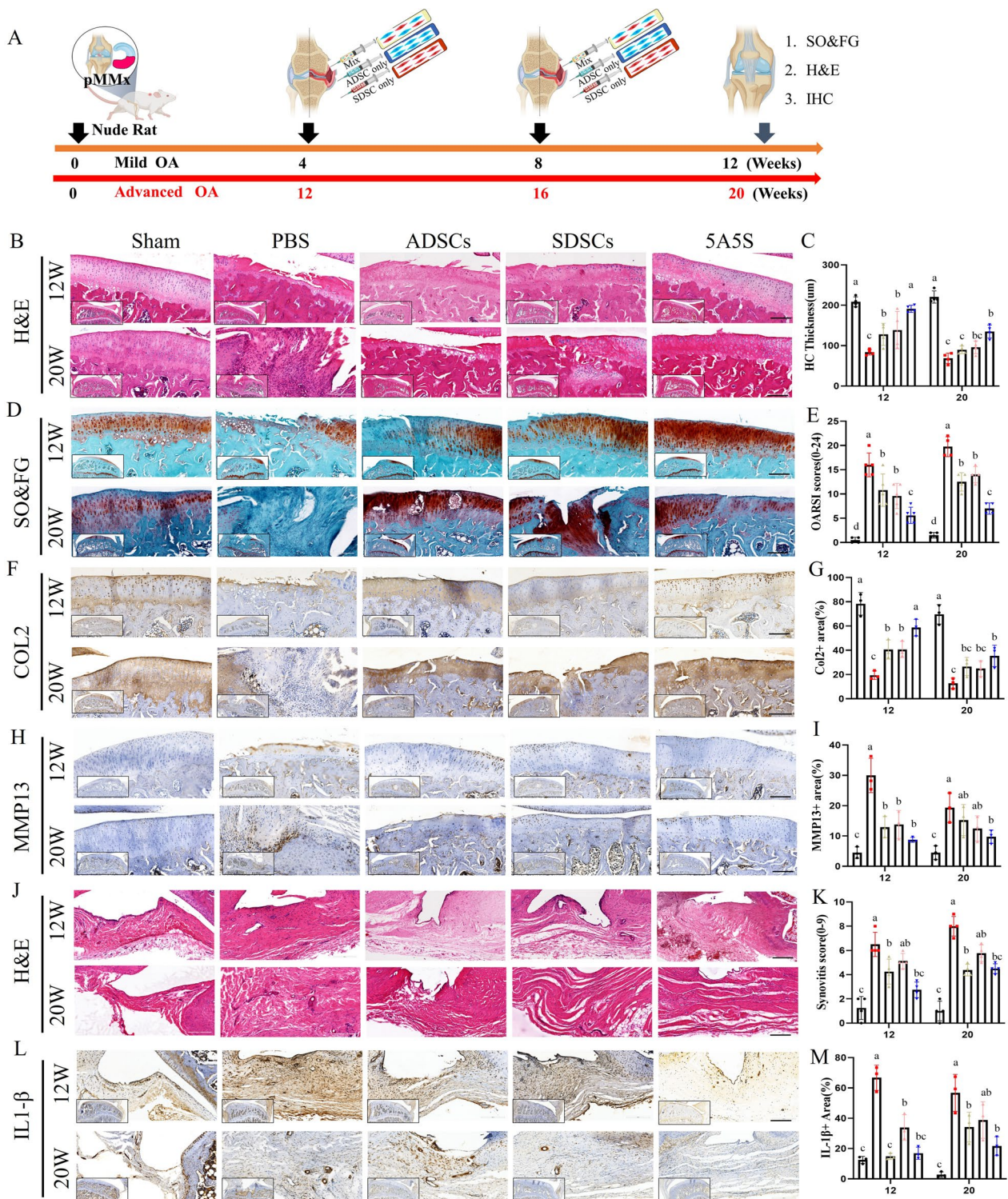


**Fig. 4** Equally combined ADSCs and SDSCs alleviated cartilage degeneration and synovial inflammation of early and advanced OA. **A** schematic illustration of intra-injection of ADSCs and SDSCs for OA therapy. **B** H&E staining and **C** hyaline cartilage thickness was evaluated. **D** Safranin O–Fast Green staining and **E** OARSI scores (n=4). **F** immunohistochemistry staining of Col2 and **G** analysis of the proportion of positive area of Col2 (n=3). **H** immunohistochemistry staining of MMP13 and **I** analysis of the proportion of MMP13 positive cell (n=3). **J** H&E staining and **K** synovial inflammation scores (n=4). **L** immunohistochemistry staining of IL-1β and **M** analysis of the proportion of IL-1β positive cell (n=3)

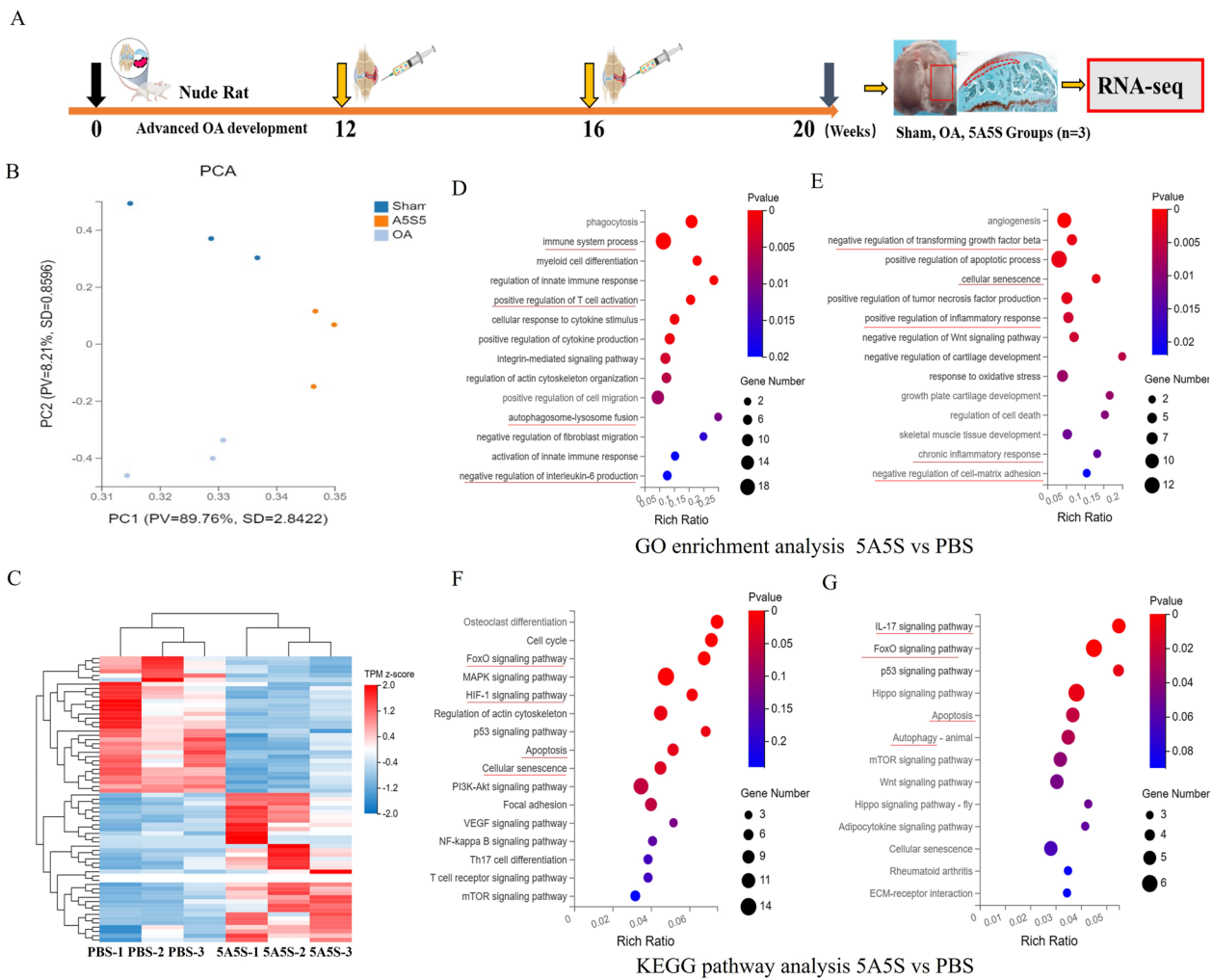


**Fig. 5** RNA-seq analysis for articular cartilage after combining ADSCs and SDSCs treatments. **A** schematic illustration of for cartilage transcriptome in Sham, PBS and 5A5S groups at 20 weeks. **B** principal component analysis. **C** hierarchical cluster analysis of genes differentially expressed in the cartilage among the 5A5S, PBS, and sham groups. Gene ontology and KEGG analysis of up-regulated (**D, F**) and down-regulated DEGs (**E, G**) in the 5A5S and PBS groups

in the 5A5S group compared with the PBS group, indicating substantial difference in therapeutic mechanism (Fig. 5C, Supplementary excel 1). Next, GO enrichment analysis revealed immune system process, positive regulation of T cell activation, autophagosome–lysosome fusion enrichment in the up-regulated DEGs (Fig. 5D); negative regulation of transforming growth factor-β (TGF-β) and cartilage development, positive regulation of inflammatory response, TNF production and chronic inflammatory response in down-regulated DEGs (Fig. 5E). KEGG pathway enrichment analysis indicated that FoxO signaling pathway enriched in the up-regulated and down-regulated DEGs (Fig. 5F, G), which was closely related to the autophagy and apoptosis of chondrocytes [30, 31]. The in vivo results further showed that

chondrocyte autophagy and FoxO signaling pathway may were involved in the cartilage regeneration in advanced OA in treatments combining ADSCs and SDSCs.

**Combined treatment with ADSCs and SDSCs relieved IL-1β-induced chondrocyte degradation, inflammation, and autophagy**

After OA chondrocytes induced by IL-1β for 48 h, the conditioned medium from ADSCs, SDSCs or 5A5S were changed to treatment OA chondrocytes for 72 h. We found that 5A5S group reduced IL-1β-induced loss in proteoglycan in high-density chondrocyte micromass by alcian blue staining (Fig. 6A). Meanwhile, changes in the protein expression of Col2 or MMP13 induced by IL-1β were clearly reversed by 5A5S (Fig. 6B, C, D).

The levels of pro-inflammatory factors IL-1 $\beta$  and TNF- $\alpha$  and anti-inflammatory factor IL-10 in the medium were analyzed by ELISA kit. The results showed that TNF- $\alpha$  and IL-1 $\beta$  levels were lower in the ADSCs-only and 5A5S groups, whereas IL-10 levels were higher in the ADSCs and 5A5S groups than those in the chondrocyte-only group (Fig. 6E). Next, from the TEM images, the autophagosome and the autolysosome dramatically increased in the 5A5S group compared with those in the control group (Fig. 6F). Moreover, autophagy activity was considerably enhanced by 5A5S, including increased percentage of the cells with LC3B puncta (Fig. 6G, J), up-regulation of the ratio of LC II to I, down-regulation of the P62 protein (Fig. 6H, K), and an increase in the puncta of autophagosome of chondrocytes by MDC staining (Fig. 6I, L). These findings further demonstrated the important role of autophagy in mediating cartilage regeneration by combined ADSCs and SDSCs.

#### Combined treatment with ADSCs and SDSCs activated chondrocyte autophagy through the FoxO1 signaling pathway

The potential of the FoxO signaling pathway in inhibiting cartilage degradation by 5A5S was studied. The 5A5S group promoted the expression of FoxO1 protein, but not phosphorylation of FoxO1 and FoxO3 (Fig. 7A, B, Fig. S6A, B). After OA chondrocytes cultured with the conditioned media from 5A5S with or without of FoxO1 inhibitor AS184285 for 72 h. The expression levels of Col2, LCII, and FoxO1 (Fig. 7C, D, E), and the puncta of autophagosome (Fig. 7F, G) considerably increased in the 5A5S group. Those levels were greatly down-regulated in the 5A5S group with the FoxO1 inhibitor. In addition, the expression levels of MMP13 and P62 considerably decreased in the 5A5S group. By contrast, the expression levels of MMP13 and P62 were up-regulated in the 5A5S group with the FoxO1 inhibitor (Fig. 7C, D, E). These data suggested that blocking FoxO1 partially attenuated the activation of autophagy and chondrogenesis induced by combined ADSCs and SDSCs. The FoxO1 signaling way was mainly responsible for activating autophagy.

## Discussion

Combined human ADSCs and SDSCs cocultured with OA chondrocyte in vitro and intra-articular injection in early and advanced OA, to assess the therapeutic efficacy. Notably, a 50/50 mixture of ADSCs and SDSCs considerably synergistically alleviated advanced OA progression, outperforming ADSCs or SDSCs alone, including reduced cartilage degeneration, reduced bone remodeling and nerve invasion in the subchondral bone. Furthermore, we discovered that combining ADSCs and SDSCs can synergistically enhance chondrogenesis by activating OA chondrocyte autophagy via the FoxO1 signal pathway (Fig. 7H).

Inflammation and articular cartilage degradation induced the progression and severity of OA symptoms. The initial inflammatory response and its induced catabolism in OA may impede cartilage repair [15, 23]. IL-1 $\beta$  or synovial fluid from advanced OA negatively affects the chondrogenic response of human MSCs, resulting in the increased expression of pro-inflammatory cytokines and cartilage-degrading enzymes [32]. Our study found that ADSCs reduced TNF- $\alpha$  and IL-1 $\beta$  levels in the OA chondrocyte and IL-1 $\beta$  positive cells in OA rats' synovium. This result was consistent with a previous study showed that ADSCs have anti-inflammatory properties in chondrocytes and synoviocytes [33]. ADSCs prevent OA chondrocytes and synovial cells producing TNF- $\alpha$  and IL-6 [33]. As a result, ADSCs' immunomodulatory and anti-inflammatory properties create a favorable environment for cartilage tissue regeneration [3].

In recent years, researchers have focused on SDSCs as a promising avenue for facilitating long-term repair and regeneration processes [23, 34]. A two-year clinical follow-up study demonstrated that SDSCs can mediate regenerative cartilage repair without causing adverse events [35]. Furthermore, the direct coculture of human chondrocytes and SDSCs promotes chondrogenesis in vitro [36]. Notably, SDSCs from patients with OA or rheumatoid arthritis demonstrated chondrogenic differentiation and regeneration ability comparable to those from patients with ACL injury [34]. In conclusion, SDSCs show promise as replacements for chondrocytes in situ, allowing cartilage regeneration in patients with extensive osteoarthritic lesions.

(See figure on next page.)

**Fig. 6** Combined ADSCs and SDSCs inhibited chondrocyte degradation and enhanced autophagy. **A** chondrocyte micromass by Alcian Blue staining. Cell immunofluorescence (**B**) and Western blot (**C**) for Col2 and MMP13 were quantitatively analyzed by gray value (**D**) ( $n=3$ ). **E** the levels of inflammatory factors IL-10 and TNF- $\alpha$  and IL-1 $\beta$  were determined by ELISA. **F** TEM analysis showing autophagosomes (arrowed). **G** Cell immunofluorescence for LC3II and **J** the proportion of cells with LC3B puncta. Western blot (**H**) for LC3II/I and P62 were quantitatively analyzed by gray value (**K**). **I, L** autophagosome in chondrocytes by MDC staining and puncta were quantitated ( $n=25$ ). All data are shown as the mean  $\pm$  SD. #denotes compared with control, ## $P < 0.01$ , ### $P < 0.001$ ; \* denotes compared with IL-1 $\beta$ , \* $P < 0.05$ , \*\* $P < 0.01$ , \*\*\* $P < 0.001$

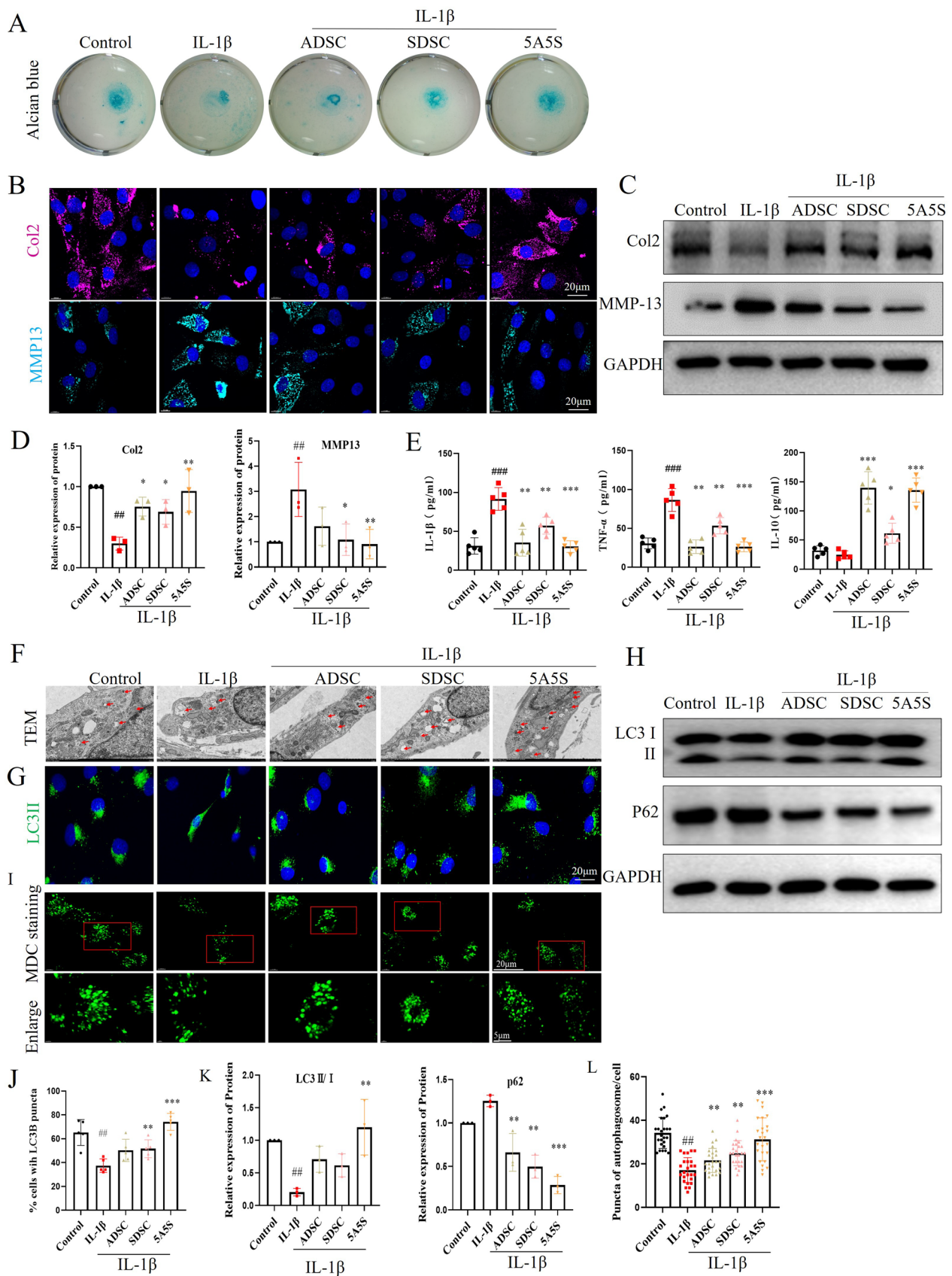


**Fig. 6** (See legend on previous page.)

Several recent studies have highlighted the benefits of combining cell therapy in the treatment of OA in animal models and clinical trials [37, 38]. Liu et al. found that administering ADSCs and SDSCs in a 1:1 ratio alleviated OA in rats by decreasing the reactive oxygen species in chondrocyte and inhibiting inflammatory responses [37]. Furthermore, Prasad et al. proposed that BMSCs and chondrocytes in a 1:1 ratio have a highly chondroprotective approach than treatments with only chondrocytes or BMSCs, in term of promoting the regeneration of damaged cartilage [38]. Subchondral cysts or bone marrow lesions have been identified as secondary phenomena associated with pain symptoms in OA [39]. Several studies have highlighted the role of activated osteoclasts in subchondral bone cysts in inducing CGPR+ sensory innervation and pain in OA [40, 41]. Therefore, interventions aimed at reducing cysts or bone marrow lesions have the potential to attenuate OA-related pain [42]. In this study showed that ADSCs and SDSCs treatment in a 1:1 ratio reduced subchondral bone marrow lesions or cysts and improved pain threshold and gait in rats. This synergistic effect may reduce the dose and frequency of injection of stem cells alone. Clinical trials have shown that higher doses ( $1 \times 10^8$  cells) of autologous BMSCs or ADSCs result in greater pain relief and more sustainable reparative effects than lower doses ( $1 \times 10^7$  cells) [43, 44]. Furthermore, repeated or periodic weekly MSCs injections have been shown to be superior to single MSCs injections in terms of pain relief and functional improvement in both animal models [45] and clinic trial [46].

It was interesting that pelleting chondrocyte, ADSCs and SDSCs together showed a higher ratio of ADSCs being more advantageous on cartilage tissue formation (Fig. S2), but the transwell co-culture tests showed equal ratio of ADSCs and SDSCs being best group (Fig. 1F, G). However, these findings were based on two individual systems respectively, transwell coculture system performs its functions mainly through secreting cytokines, while cell-to-cell contact and paracrine effects play an important role in pelleting coculture system [47]. Given that ADSCs and SDSCs primarily localize to the synovial membrane and meniscus surface after injection, their ability to stimulate tissue regeneration was primarily

mediated through paracrine mechanisms. The paracrine factors secreted by MSCs exhibit a high degree of complexity and diversity, comprising a range of factors, such as TGF- $\beta$ , fibroblast growth factors. As RNA-seq results showed the FGF binding proteins (FGFBPs) significantly high expression after combined ADSCs and SDSCs treatment, FGFBPs mobilized FGFs to their cognate receptors and stored in the extracellular matrix [48]. These factors contribute to chondrogenic differentiation capabilities and anti-inflammatory effects [49]. Maumus et al. demonstrated that ADSCs inhibit apoptosis and reduce the expression of hypertrophic markers through the secretion of hepatocyte growth factor [50]. Chau et al. found that synoviocytes secrete factors that promote articular cartilage formation and inhibit chondrocytic hypertrophic differentiation [51]. Understanding the mechanisms underlying the actions of paracrine factors will be instrumental in strategies that can impede the progression of cartilage degeneration and in the refinement of therapies [52].

Autophagy activation, which is a self-protective mechanism in chondrocytes, improves chondrocyte viability and impedes the progression of OA [53]. Normal chondrocytes express autophagy-related proteins, including ULK1, beclin-1, and LC3-II [54], but a large number of autophagy proteins decreased in the late stage of OA or in the cartilage of elderly people [55]. The inhibition of chondrocyte autophagy promoted *MMP13* and *ADAMTS5* gene expression in chondrocytes and decreased *COL2A1* gene expression. The decrease in autophagy leads to the accumulation of intracellular damaged organelles and macromolecules in chondrocytes, reducing the survival of chondrocytes and ultimately leading to age-related OA [56]. Promoting autophagy can slow down cartilage degeneration in OA [57]. For example, intra-articular injection of rapamycin enhances chondrocyte autophagy, thereby delaying the progression of OA by inhibiting chondrocyte apoptosis and senescence [58, 59]. Furthermore, local intra-articular rapamycin activates autophagy, and decrease *MMP13* and *Col10* levels, and alleviates cartilage destruction in rodents [58]. The activation of autophagy inhibits the release of IL-1 $\beta$ -induced

(See figure on next page.)

**Fig. 7** FoxO1 inhibitor weakened the enhanced autophagy induced by ADSCs and SDSCs. **A** p-FoxO1 and FoxO1 by Western blot and **(B)** the quantitative analysis of the bands. **C** cell immunofluorescence for Col2, MMP13, LC3II, and DAPI. **D** Western blot for Col2, MMP13, LC3II/I, P62, and FoxO1 were quantitatively analyzed by gray value **(E)** ( $n=3$ ). **F** The autophagosome in chondrocytes by MDC staining and puncta were quantified **(G)** ( $n=25$ ). **H** Schematic illustration of mechanism of combined ADSCs and SDSCs attenuated severe OA progression, including attenuated cartilage degeneration and enhanced autophagy by activating the FoxO1 signaling pathway, relieved bone remodeling and nerve invasion in subchondral bone, decreased osteophyte formation, and suppressed synovial inflammation. (All data are shown as the mean  $\pm$  SD. #denotes compared with control, ## $P < 0.01$ ; \* denotes compared with 5A5S, \* $P < 0.05$ , \*\* $P < 0.01$ , \*\*\* $P < 0.001$ )

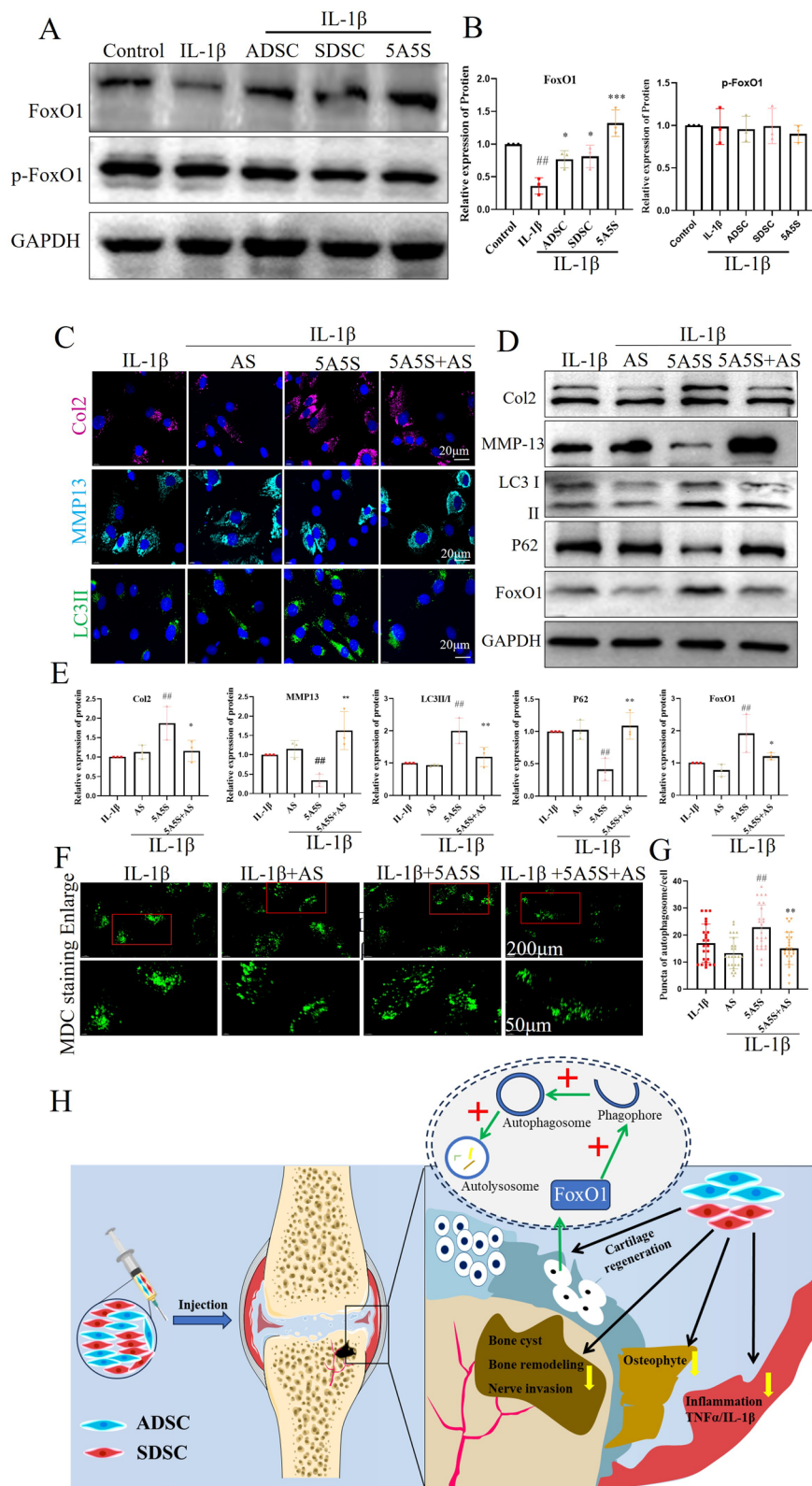


**Fig. 7** (See legend on previous page.)

inflammatory factors and the production of MMPs and decreases synovial inflammation and subchondral osteosclerosis [60, 61]. Our findings suggested that combined treatment with human MSCs stimulated OA chondrocyte autophagy and autophagy flux, potentially slowing or even reversing disease progression. Interestingly, ADSCs activate autophagy and inhibit IL-1 $\beta$ -induced inflammation in human chondrocytes [33, 62]. Therefore, the activation of autophagy of degenerative chondrocytes may be an effective method for impeding the degeneration of articular cartilage [63].

The mechanisms involved in autophagy activation mainly depend on the mTOR and FoxO1 pathways. Our RNA-sequencing analysis identified the FoxO signaling pathway as the most up-regulated in the cartilage treated with both human MSCs. These findings are consistent with recent reports identifying FoxO1 as a key player in articular chondrocyte homeostasis, making it a potential therapeutic target for OA [64]. The overexpression of FoxO1 reduces inflammation and cartilage-degrading enzymes by promoting autophagy [60], reduces inflammatory mediators and chondro-degrading enzymes, promotes the expression of autophagy-related genes, such as *LC3-II*, and provides protection against IL-1 $\beta$  induction [60, 65]. TGF- $\beta$ 1 promoted the protein expression of FoxO1 and nuclear translocation of FoxO1 [64]. FoxO1 in the nucleus directly binds gene promoters to activate autophagy-related genes, including *Beclin-1* and *LC3-II*. The transcription-dependent regulation of autophagy activated by FoxO1 directly binding to gene promoter is essential for the complement of autophagy proteins, enabling autophagy to function normally [64]. Combined treatment with ADSCs and SDSCs effectively promoted the expression of FoxO1 in the OA chondrocytes induced by IL-1 $\beta$ . AS1842856, which reduces the activity of FoxO1 by binding to FoxO1 [66], can reverse the effects of the combined treatment. Moreover, the combined treatment may activate the transcription of autophagy through intranuclear FoxO1. However, the role of FoxO1 in autophagy induced by the combined treatment needs to be further elucidated.

Our study has several limitations that must be acknowledged. To begin, more large-animal studies and clinical trials are needed to thoroughly assess the preclinical safety and efficacy of combined stem cell therapies. Our study used bilateral OA model of immunodeficient rats to avoid potential rejection of human-derived stem cells, but it was exponentially more difficult to evaluate the gait parameters due to weight bearing asymmetry [67]. Furthermore, direct evidences of what exact factors are secreted by combined stem cells involved in cartilage regeneration were not carried out, which required further investigation.

## Conclusion

Our findings suggested that administering equal proportions of human ADSCs and SDSCs via articular injection has a synergistic effect, resulting in anti-inflammatory and chondroprotective effects in early and advanced OA. The aforementioned effects were found to be achieved through increased chondrocyte autophagy via the FoxO1 signaling pathway.

## Supplementary Information

The online version contains supplementary material available at <https://doi.org/10.1186/s13287-024-03870-6>.

Additional file1 (DOCX 9155 KB)

Additional file2 (XLSX 47 KB)

## Acknowledgements

We acknowledge the assistance of Ying Wang for the micro-CT imaging from the SUSTech Research Core. The authors declared that artificial intelligence was not used in this study.

## Author contributions

WJQ, LGH, LC participated in design of the study, performed the statistical analysis. WJQ performed animal experiments and drafted the manuscript. H SQ and LQ performed the cell experiments. LQS and LY prepared and identified of stem cells. LK provided fluorescent nanoparticles (FNPs) and assisted cell tracking. LGH, LC, YYY participated in editing the manuscript. D WF and L G-ANG collected human tissue samples and animal experiments. YH P analyzed the RAN-seq data.

## Funding

This work was supported by grants from the National Natural Science Foundation of China (82172463), Shenzhen Science and Technology Innovation Commission (JCYJ20190809114209434, KQTD20200820113012029) and Guangdong Provincial Key Laboratory of Advanced Biomaterials (2022B1212010003).

## Data availability

All experimental protocols and data obtained in this study were available upon request to the corresponding author. All the data supporting the conclusions of this study are included within the article and supplementary data.

## Declarations

### Ethical approval

The procedure for obtaining human tissue samples from hospitals was approved by the medical ethics committee of Shenzhen People's Hospital (Approval Number: LL-KY-2021069; Title: Clinical investigation of mixed ADSCs and SDSCs for the treatment of human knee osteoarthritis by local joint injection; Date of approval: 01/03/2021). All the patients have signed informed consent forms for the use of the tissue samples. All experimental and animal care procedures were approved by Southern University of Science and Technology (Approval Number: SUSTech-SL2021112901; Title: The mechanism of combined human-derived ADSCs and SDSCs for the treatment of knee osteoarthritis, Date of approval: 12/01/2021).

### Consent for publication

All authors have read and approved the final version of the manuscript.

### Competing interests

The authors declare no conflicts of financial interest.

### Author details

<sup>1</sup>Division of Adult Joint Reconstruction and Sports Medicine, Department of Orthopedic Surgery, The First Affiliated Hospital (Shenzhen People's Hospital), School of Medicine, Southern University of Science and Technology, 1017

Dongmen North Road, Luohu District, Shenzhen 518055, China. <sup>2</sup>Shenzhen Key Laboratory of Musculoskeletal Tissue Reconstruction and Function Restoration, Shenzhen People's Hospital, Guangdong, China. <sup>3</sup>School of Biomedical Sciences, Hunan University, Changsha 410082, Hunan, China. <sup>4</sup>Department of Biomedical Engineering, College of Engineering, Southern University of Science and Technology, 1088 Xueyuan Avenue, Nanshan District, Shenzhen 518055, Guangdong, China. <sup>5</sup>Guangdong Provincial Key Laboratory of Advanced Biomaterials, Southern University of Science and Technology, Shenzhen, Guangdong, China.

Received: 19 February 2024 Accepted: 30 July 2024  
Published online: 15 August 2024

## References

- Sharma L. Osteoarthritis of the Knee. *N Engl J Med.* 2021;384:51–9.
- Yao Q, et al. Osteoarthritis: pathogenic signaling pathways and therapeutic targets. *Signal Transduct Target Ther.* 2023;8:56.
- Muthu S, et al. Failure of cartilage regeneration: emerging hypotheses and related therapeutic strategies. *Nat Rev Rheumatol.* 2023;19:403–16.
- Hodgkinson T, Kelly DC, Curtin CM, O'Brien FJ. Mechanosignalling in cartilage: an emerging target for the treatment of osteoarthritis. *Nat Rev Rheumatol.* 2022;18:67–84.
- Kwon DG, et al. State of the art: the immunomodulatory role of MSCs for osteoarthritis. *Int J Mol Sci.* 2022;23(3):1618.
- Copp G, Robb KP, Viswanathan S. Culture-expanded mesenchymal stromal cell therapy: Does it work in knee osteoarthritis? A pathway to clinical success. *Cell Mol Immunol.* 2023;20:626–50.
- Wiggers TG, Winters M, Van den Boom NA, Haisma HJ, Moen MH. Autologous stem cell therapy in knee osteoarthritis: a systematic review of randomised controlled trials. *Br J Sports Med.* 2021;55:1161–9.
- Iijima H, Isho T, Kuroki H, Takahashi M, Aoyama T. Effectiveness of mesenchymal stem cells for treating patients with knee osteoarthritis: a meta-analysis toward the establishment of effective regenerative rehabilitation. *NPJ Regen Med.* 2018;3:15.
- Lamo-Espinosa JM, et al. Long-term efficacy of autologous bone marrow mesenchymal stromal cells for treatment of knee osteoarthritis. *J Transl Med.* 2021;19:506.
- Kim KI, et al. Clinical efficacy and safety of the intra-articular injection of autologous adipose-derived mesenchymal stem cells for knee osteoarthritis: a phase III, randomized, double-blind, Placebo-Controlled Trial. *Am J Sports Med.* 2023;51:2243–53.
- Sekiya I, Muneta T, Horie M, Koga H. Arthroscopic transplantation of synovial stem cells improves clinical outcomes in knees with cartilage defects. *Clin Orthop Relat Res.* 2015;473:2316–26.
- Yoshimura H, et al. Comparison of rat mesenchymal stem cells derived from bone marrow, synovium, periosteum, adipose tissue, and muscle. *Cell Tissue Res.* 2007;327:449–62.
- Zha K, et al. Heterogeneity of mesenchymal stem cells in cartilage regeneration: from characterization to application. *NPJ Regen Med.* 2021;6:14.
- Veronesi F, et al. Evaluation of cartilage biomechanics and knee joint microenvironment after different cell-based treatments in a sheep model of early osteoarthritis. *Int Orthop.* 2021;45:427–35.
- Bhattacharjee M, et al. Injectable amnion hydrogel-mediated delivery of adipose-derived stem cells for osteoarthritis treatment. *Proc Natl Acad Sci USA.* 2022. <https://doi.org/10.1073/pnas.2120968119>.
- Sadri B, et al. Cartilage regeneration and inflammation modulation in knee osteoarthritis following injection of allogeneic adipose-derived mesenchymal stromal cells: a phase II, triple-blinded, placebo controlled, randomized trial. *Stem Cell Res Ther.* 2023;14:162.
- Sakaguchi Y, Sekiya I, Yagishita K, Muneta T. Comparison of human stem cells derived from various mesenchymal tissues: superiority of synovium as a cell source. *Arthritis Rheum.* 2005;52:2521–9.
- Futami I, et al. Isolation and characterization of multipotential mesenchymal cells from the mouse synovium. *PLoS ONE.* 2012;7:e45517.
- Ma Y, et al. Anti-hypertrophic effect of synovium-derived stromal cells on costal chondrocytes promotes cartilage repairs. *J Orthop Translat.* 2022;32:59–68.
- Akgun I, et al. Matrix-induced autologous mesenchymal stem cell implantation versus matrix-induced autologous chondrocyte implantation in the treatment of chondral defects of the knee: a 2-year randomized study. *Arch Orthop Trauma Surg.* 2015;135:251–63.
- Mayet A, Zablotski Y, Roth SP, Brehm W, Troillet A. Systematic review and meta-analysis of positive long-term effects after intra-articular administration of orthobiologic therapeutics in horses with naturally occurring osteoarthritis. *Front Vet Sci.* 2023;10:1125695.
- Gonzalez-Fernandez P, Rodríguez-Nogales C, Jordan O, Allémann E. Combination of mesenchymal stem cells and bioactive molecules in hydrogels for osteoarthritis treatment. *Eur J Pharm Biopharm.* 2022;172:41–52.
- McGonagle D, Baboolal TG, Jones E. Native joint-resident mesenchymal stem cells for cartilage repair in osteoarthritis. *Nat Rev Rheumatol.* 2017;13:719–30.
- Neybecker P, et al. In vitro and in vivo potentialities for cartilage repair from human advanced knee osteoarthritis synovial fluid-derived mesenchymal stem cells. *Stem Cell Res Ther.* 2018;9:329.
- Goshima A, et al. Basic fibroblast growth factor promotes meniscus regeneration through the cultivation of synovial mesenchymal stem cells via the CXCL6-CXCR2 pathway. *Osteoarthr Cartil.* 2023;31:1581–93.
- Zhou W, et al. Single-cell profiles and clinically useful properties of human mesenchymal stem cells of adipose and bone marrow origin. *Am J Sports Med.* 2019;47:1722–33.
- Yan X, et al. Anti-friction MSCs delivery system improves the therapy for severe osteoarthritis. *Adv Mater.* 2021;33:e2104758.
- Pritzker KP, et al. Osteoarthritis cartilage histopathology: grading and staging. *Osteoarthr Cartil.* 2006;14:13–29.
- Yang C, et al. Single-cell spatiotemporal analysis reveals cell fates and functions of transplanted mesenchymal stromal cells during bone repair. *Stem Cell Rep.* 2022;17(10):2318–33.
- Lee KI, et al. FOXO1 and FOXO3 transcription factors have unique functions in meniscus development and homeostasis during aging and osteoarthritis. *Proc Natl Acad Sci USA.* 2020;117:3135–43.
- Matsuzaki T, et al. FoxO transcription factors modulate autophagy and proteoglycan 4 in cartilage homeostasis and osteoarthritis. *Sci Transl Med.* 2018. <https://doi.org/10.1126/scitranslmed.aan0746>.
- Gómez-Aristizábal A, et al. Stage-specific differences in secretory profile of mesenchymal stromal cells (MSCs) subjected to early- vs late-stage OA synovial fluid. *Osteoarthr Cartil.* 2017;25:737–41.
- Jiang LB, et al. Adipose-derived stem cells induce autophagic activation and inhibit catabolic response to pro-inflammatory cytokines in rat chondrocytes. *Osteoarthr Cartil.* 2016;24:1071–81.
- Koizumi K, et al. Synovial mesenchymal stem cells from osteo- or rheumatoid arthritis joints exhibit good potential for cartilage repair using a scaffold-free tissue engineering approach. *Osteoarthr Cartil.* 2016;24:1413–22.
- Shimomura K, et al. First-in-human pilot study of implantation of a scaffold-free tissue-engineered construct generated from autologous synovial mesenchymal stem cells for repair of knee chondral lesions. *Am J Sports Med.* 2018;46:2384–93.
- Kim TW, Lee MC, Bae HC, Han HS. Direct coculture of human chondrocytes and synovium-derived stem cells enhances in vitro chondrogenesis. *Cell J.* 2018;20:53–60.
- Liu X, Liu Y, He H, Xiang W, He C. Human adipose and synovial mesenchymal stem cells improve osteoarthritis in rats by reducing chondrocyte reactive oxygen species and inhibiting inflammatory response. *J Clin Lab Anal.* 2022;36:e24353.
- Prasadam I, et al. Mixed cell therapy of bone marrow-derived mesenchymal stem cells and articular cartilage chondrocytes ameliorates osteoarthritis development. *Lab Invest.* 2018;98:106–16.
- Perry TA, et al. Magnetic resonance imaging-assessed subchondral cysts and incident knee pain and knee osteoarthritis: data from the multi-center osteoarthritis study. *Arthritis Rheumatol.* 2022;74:60–9.
- Zhu S, et al. Subchondral bone osteoclasts induce sensory innervation and osteoarthritis pain. *J Clin Invest.* 2019;129:1076–93.
- Zhou F, et al. Associations of osteoclastogenesis and nerve growth in subchondral bone marrow lesions with clinical symptoms in knee osteoarthritis. *J Orthop Translat.* 2022;32:69–76.
- Wu J, et al. Axial compressive loading attenuates early osteoarthritis by reducing subchondral bone remodeling. *Am J Sports Med.* 2023;51:1752–64.
- Lamo-Espinosa JM, et al. Intra-articular injection of two different doses of autologous bone marrow mesenchymal stem cells versus hyaluronic



- acid in the treatment of knee osteoarthritis: multicenter randomized controlled clinical trial (phase I/II). *J Transl Med.* 2016;14:246.
44. Jo CH, et al. Intra-articular injection of mesenchymal stem cells for the treatment of osteoarthritis of the knee: a proof-of-concept clinical trial. *Stem Cells.* 2014;32:1254–66.
  45. Ozeki N, et al. Not single but periodic injections of synovial mesenchymal stem cells maintain viable cells in knees and inhibit osteoarthritis progression in rats. *Osteoarthr Cartil.* 2016;24:1061–70.
  46. Matas J, et al. Umbilical cord-derived mesenchymal stromal cells (MSCs) for knee osteoarthritis: repeated MSC dosing is superior to a single MSC dose and to hyaluronic acid in a controlled randomized phase I/II trial. *Stem Cells Transl Med.* 2019;8:215–24.
  47. Bian Y, et al. A comparative study of HAMSCs/HBMSCs transwell and mixed coculture systems. *IUBMB Life.* 2019;71:1048–55.
  48. Schmidt MO, et al. The role of fibroblast growth factor-binding protein 1 in skin carcinogenesis and inflammation. *J Invest Dermatol.* 2018;138:179–88.
  49. Zhong L, Huang X, Karperien M, Post JN. The regulatory role of signaling crosstalk in hypertrophy of MSCs and human articular chondrocytes. *Int J Mol Sci.* 2015;16:19225–47.
  50. Maumus M, et al. Adipose mesenchymal stem cells protect chondrocytes from degeneration associated with osteoarthritis. *Stem Cell Res.* 2013;11:834–44.
  51. Chau M, et al. The synovial microenvironment suppresses chondrocyte hypertrophy and promotes articular chondrocyte differentiation. *NPJ Regen Med.* 2022;7:51.
  52. Li MH, Xiao R, Li JB, Zhu Q. Regenerative approaches for cartilage repair in the treatment of osteoarthritis. *Osteoarthr Cartil.* 2017;25:1577–87.
  53. Caramés B, et al. Autophagy activation by rapamycin reduces severity of experimental osteoarthritis. *Ann Rheum Dis.* 2012;71:575–81.
  54. Zhang Y, et al. Cartilage-specific deletion of mTOR upregulates autophagy and protects mice from osteoarthritis. *Ann Rheum Dis.* 2015;74:1432–40.
  55. Vinatier C, Domínguez E, Guicheux J, Caramés B. Role of the inflammation-autophagy-senescence integrative network in osteoarthritis. *Front Physiol.* 2018;9:706.
  56. Boudérique T, et al. Targeted deletion of Atg5 in chondrocytes promotes age-related osteoarthritis. *Ann Rheum Dis.* 2016;75:627–31.
  57. Jin Z, et al. Curcumin exerts chondroprotective effects against osteoarthritis by promoting AMPK/PINK1/Parkin-mediated mitophagy. *Biomed Pharmacother.* 2022;151: 113092.
  58. Takayama K, et al. Local intra-articular injection of rapamycin delays articular cartilage degeneration in a murine model of osteoarthritis. *Arthritis Res Ther.* 2014;16:482.
  59. Lu H, et al. Fibroblast growth factor 21 (FGF21) alleviates senescence, apoptosis, and extracellular matrix degradation in osteoarthritis via the SIRT1-mTOR signaling pathway. *Cell Death Dis.* 2021;12:865.
  60. Ohzono H, et al. Targeting FoxO transcription factors with HDAC inhibitors for the treatment of osteoarthritis. *Ann Rheum Dis.* 2023;82:262–71.
  61. Parzych KR, Kliionsky DJ. An overview of autophagy: morphology, mechanism, and regulation. *Antioxid Redox Signal.* 2014;20:460–73.
  62. Sasaki H, et al. Autophagy modulates osteoarthritis-related gene expression in human chondrocytes. *Arthritis Rheum.* 2012;64:1920–8.
  63. Lv X, et al. New insights into the interplay between autophagy and cartilage degeneration in osteoarthritis. *Front Cell Dev Biol.* 2022;10:1089668.
  64. Wang C, Shen J, Ying J, Xiao D, O’Keefe RJ. FoxO1 is a crucial mediator of TGF- $\beta$ /TAK1 signaling and protects against osteoarthritis by maintaining articular cartilage homeostasis. *Proc Natl Acad Sci U S A.* 2020;117:30488–97.
  65. Akasaki Y, et al. FoxO transcription factors support oxidative stress resistance in human chondrocytes. *Arthritis Rheumatol.* 2014;66:3349–58.
  66. Eng SJ, et al. FOXO inhibition rescues  $\alpha$ -defensin expression in human intestinal organoids. *Proc Natl Acad Sci USA.* 2023;120: e2312453120.
  67. Araya N, et al. Intra-articular Injection of pure platelet-rich plasma is the most effective treatment for joint pain by modulating synovial inflammation and calcitonin gene-related peptide expression in a rat arthritis model. *Am J Sports Med.* 2020;48:2004–12.

## Publisher’s Note

Springer Nature remains neutral with regard to jurisdictional claims in published maps and institutional affiliations.